



Design, Modeling and Experiments of An In-pipe Magnetostrictive Impact Drive Mechanism

R. Zhao^{*a,b}

^aJiangxi Province Key Laboratory of Precision Drive & Control, Nanchang Institute of Technology, Nanchang, China

^bSchool of Electrical Engineering, Hebei University of Technology, Tianjin, China

PAPER INFO

Paper history:

Received 27 August 2016

Received in revised form 14 February 2018

Accepted 14 February 2018

Keywords:

In-pipe Motor

Impact Drive Mechanism

Magnetostrictive Materials

Inertia Impact Principle

Precision Positioning

ABSTRACT

This paper presents a magnetostrictive in-pipe impact drive mechanism (IDM). To estimate the output performances of the IDM, a dynamics model was developed based on the magnetostrictive material constitutive model and mechanical model of the IDM. Therefore, an experimental system has been built to test the motion performance of IDM. Simulation and experimental results illustrate that the proposed model can accurately predict the step-size of the IDM. The working frequency of the designed IDM is from 10 to 120 Hz, with a the step-size resolution of 740 nm. The magnetostrictive IDM performs good linearity, and can be applied to precision positioning.

doi: 10.5829/ije.2018.31.05b.08

NOMENCLATURE

E	Young's modulus (GPa)	l_r	Length of Terfenol-D rod (mm)
λ_s	Saturation magnetostriction (ppm)	A_r	Areas of Terfenol-D rod (mm ²)
M_s	Saturation magnetization (kA/m)	A_m	Areas of magnetic field (mm ²)
χ_m	Initial susceptibility	N	Turns of coil
M	Magnetization (kA/m)	M	Slider mass (kg)
H	Magnetic field intensity (kA/m)	m	Counter mass (kg)
B	Magnetic flux density (T)	v_s	Stribeck velocity (m/s)
k	Relaxation factor	σ_0	Average stiffness of bristles (N/m)
σ	Stress (N)	σ_1	Damping frictional coefficient (N·s/m)
ε	Strain (ppm)	σ_2	Viscous frictional coefficient (N·s/m)
μ	Permittivity (H/m)	τ_c	Coulomb friction coefficient
μ_r	Relative permeability	τ_s	Sliding friction coefficient
I	Current (A)		
f	Frequency (Hz)		

1. INTRODUCTION

Nowadays, the precision positioning devices, such as scanning displacement devices, ultrasonic motors and impact driving mechanism, are widely used in optics, biology, robot, machining industries [1-4]. IDM, based on inertial impact principle to realize the stepping motion, is one of the most common precision positioning device.

In the last three decades, with the developing of smart materials, shape memory alloy (SMA) and piezoelectric (PZ) materials have been applied to a lot of intellectual structures [5-7], and the same in IDMs [8-10]. Among them, piezoelectric materials have advantages of fast response, high accuracy and simply controlling, thus the piezoelectric IDMs have been applied to anti-shaking cameras and robots [11, 12]. However, there are still limited by the low energy density and small output force. Terfenol-D seems like can resolve these

*Corresponding Author Email: zhaoran@nit.edu.cn (R. Zhao)

problems. Its strain coefficient is 1000-2000 ppm ever reported.

Some researchers have been reported that the applications of magnetostrictive materials (MS) in the rotary and linear motion devices. Zhou developed a magnetostrictive rotary motor based on Terfenol-D rod [13]. Kim presented a linear magnetostrictive motor with three-phase excitation [14]. These motors display good performances in large output force, low exciting voltage and long-life. But there are still some disadvantages of them. Firstly, a multiturn coil is required to provide a large magnetic field for Terfenol-D rod. In the meantime, to reduce the magnetic flux leakage, an actuator housing is generally needed to provide a closed magnetic circuit. By this way, the volume of IDM will be very large, and the thermal losses causing by the coil will decrease the positioning accuracy of IDM. Secondly, a guide rail is necessary to help the IDM moving straightly [9, 15, 16], but this structure brings difficulty for locating and fixing of the IDM.

In our work, an in-pipe MS-IDM with compact construction was developed. Then, the design and model of the given motor were discussed. At last, an experimental system was built to test the motion behavior of the proposed IDM. More details are shown in the following sections.

2. DESIGN

2. 1. Construction

The proposed magnetostrictive IDM is shown in Figure 1. As shown in Figure 1a, the IDM consists of four parts: a cylindrical guide (made of magnetic-conducting material), an exciting coil, a Terfenol-D rod and a counter mass (copper). The structure of IDM is shown in Figure 1b. The Terfenol-D rod is put in a coil frame and circled by copper wires. A spring is used to provide a prestress to Terfenol-D rod, and the stress can be adjusted by the adjustment nut. Besides, a pipe type guide is utilized for IDM to replace the housing of actuator. And the guider provides a magnetic circuit for the magnetic field. The overall size of the motor is $\Phi 40 \text{ mm} \times 180 \text{ mm}$.

2. 2. Magnetostrictive Materials The Terfenol-D rod we used is manufactured by Gansu Tianxing Rare Earth Functional Materials Co. Ltd. The maximum magnetostriction the rod is 1200 ppm, with size of $\Phi 8 \text{ mm} \times 80 \text{ mm}$. The physical parameters of Terfenol-D is given in Table 1.

It is known that the change of strain with the varying magnetic field is nonlinear. To ensure the accuracy of the MS actuator, the selecting of linear region for Terfenol-D rod is necessary; that can be determined by the magnetostriction-magnetic field curve.

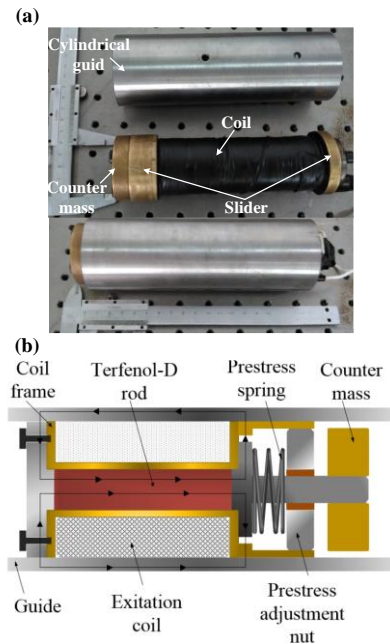


Figure 1. Construction of the magnetostrictive IDM

TABLE 1. Parameters of Terfenol-D rod

Symbol	Parameters	Value (Units)
E	Young's modulus	26.5 GPa
λ_s	Saturation magnetostriction	1200 ppm
M_s	Saturation magnetization	765 kA/m
χ^m	Initial susceptibility	110

Once the linear working region was determined, the output performance of the magnetostrictive IDM can be obtained.

3. MODEL

3. 1. Magnetic Field Model

With the compact construction (see Figure 1b), a closed magnetic circuit is formed inside the mechanism. In this way, the magnetic field analysis and calculations are easy to be implemented under the following two assumptions: (1) leakage magnetic flux and (2) actuator coil mmf loss are zero.

According to Ampere's law, the line integral of the magnetic field intensity can be expressed as,

$$\oint H dl = H_m l_m + H_r l_r \quad (1)$$

where H_m is the magnetic field intensity of the coil; l_m the length of the coil; H_r is the magnetic field of Terfenol-D rod and l_r the length of Terfenol-D rod.

Using the relationship of magnetic field H and current I , Equation (1) can be rewritten as,

$$H_m l_m + H_r l_r = NI \tag{2}$$

Then, using the constitutive relationship $B=\mu H$, Equation (2) becomes,

$$B_m l_m + (B_r / \mu_r) l_r = NI \tag{3}$$

where A_m is the area of actuator coil, A_r the area of Terfenol-D rod; μ is the magnetic permeivity, equals $\mu_0 \mu_r$.

Assuming the length of Terfenol-D rod equals that of the coil, $l_r=l_m$, and the flux in Terfenol-D rod equals that of the coil, $B_m A_m=B_r A_r$. Rearranging and substituting Equation (3) into Equation (1), we have,

$$H = \left[\frac{\mu_r}{1 + \mu_r (A_r / A_m)} \right] \left(\frac{NI}{l_r} \right) \tag{4}$$

3. 2. Magnetostrictive Constitutive Model

Experiments have testified that the magnetostrictive materials perform strong nonlinear [17]. Some of the magnetostrictive actuators can still perform a linear behavior by choosing appropriately applied magnetic field. A simple linear theory can be used to describe the Terfenol-D rod. Which are the piezomagnetic equation and the quadratic domain rotation model and given by:

$$\varepsilon = \frac{\sigma}{E} + \lambda \tag{5}$$

$$\lambda = \frac{3\lambda_s}{2M_s^2} M^2 \tag{6}$$

It is known that the relationship of magnetization and magnetic field intensity is strongly nonlinear. As one of the ferromagnetic materials, magnetization process of Terfenol-D can be described by Langevin equation [18]:

$$M = M_s \left(\coth(kH) - \frac{1}{(kH)} \right) \tag{7}$$

where $k=3\chi_m/M_s$, is the relaxation factor; χ_m the initial permeability.

According to Equation (7), relative permeability μ_r can be expresses as follow,

$$\mu_r = \frac{\coth(kH)}{H} - \frac{1}{kH^2} + 1 \tag{8}$$

3. 3. Mechanical Model

To analyze the dynamic response of the IDM, the spring-damper-mass model are usually employed to obtain the motion equations [16, 19, 20]. In the PZ-IDM system, the piezoelectric element can be regarded as an equivalent spring, as shown in Figure 2a. But it is different of PZ-IDM and MS-IDM, with the latter having an prestress spring. So we developed a more accurate model of

magnetostoeictive IDM (see Figure 2b). In this model, there are two springs of Terfenol-D rod's equivalent stiffness K_r and pre-stress spring's stiffness K_p , respectively. Also, C_r is the Terfenol-D rod damper of and C_m the counter mass damper.

The motion equations of MS-IDM shown in Figure 2b can be defined as follows:

$$\begin{cases} M\ddot{X} - C_e \dot{x} - K_e x = F_\mu - F_r \\ m(\ddot{X} + \ddot{x}) + C_e \dot{x} + K_e X = F_r \end{cases} \tag{9}$$

where M is the mass of the slider (actuator), m is the mass of counter mass; X, \dot{X} and \ddot{X} are the displacement, velocity and acceleration of the slider; x, \dot{x} and \ddot{x} are displacement, velocity and acceleration of the counter mass; C_e and K_e are the equivalent damper and stiffness; F_r is the force generated by Terfenol-D rod, F_μ is the friction force.

The equivalent equations of springs and dampers are shown as follow:

$$K_e = \frac{K_r K_p}{K_r + K_p}, C_e = C_r + C_m \tag{10}$$

where the stiffness coefficient K_r equals EA_r/l_r .

According to Equations (7), (8) and $\varepsilon l_r = EA_r$, the output force F_r of Terfenol-D rod can be set as,

$$F_r = \frac{3EA_r}{2l_r M_s^2} \left[\frac{(\mu_r - 1)\mu_r}{1 + \mu_r (A_r / A_m)} \cdot \frac{NI}{l_r} \right]^2 \tag{11}$$

The LuGre Model [20, 21] is employed to describe the friction force, which is described as follows:

$$\begin{cases} \dot{F}_r = \sigma_0 z + \sigma_1 \frac{dz}{dt} + \sigma_2 \dot{X} \\ \frac{dz}{dt} = \dot{X} - \frac{|\dot{X}|}{g(\dot{X})} z \end{cases} \tag{12}$$

where z is the average deflection of the bristles; σ_0, σ_1 and σ_2 are the stiffness, the damping static friction coefficient and the viscous friction coefficient, respectively; function $g(\dot{X})$ can be determined by Stribeck effect, the expression is $\sigma_0 g(\dot{X}) = [\tau_c + (\tau_s - \tau_c) \cdot \exp(-|\dot{X}|/v_s)](m_1 + m_2)g$.

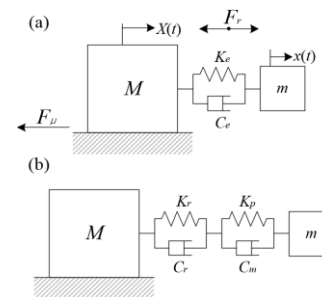


Figure 2. Mechanical model of (a) Spring-damper-mass model for PZ-IDM and (b) Accurate model for MS-IDM

Here τ_c is the Coulomb friction coefficient, τ_s is the sliding friction coefficient and v_s is the Stribeck viscosity.

3. 4. Step-size Prediction Model By resolving Equation set (9), we can get the step-size prediction formula as,

$$X(t) = (m_1 + m_2) \left(A_1 \sin(\omega_d t + A_2) e^{-\xi \omega_n t} - A_3 \right) F_r + m_2 \left(A_4 t^2 + A_3 - A_1 \sin(\omega_d t + A_2) e^{-\xi \omega_n t} \right) F_\mu \quad (13)$$

where,

$$A_1 = \frac{m}{K_e(M+m)} \sqrt{\left(\frac{C_e}{M+m}\right)^2 + \left(\frac{m}{M+m}\right)^2}$$

$$A_2 = \tan^{-1}\left(\frac{2Mm\omega_d}{C_e(M+m)}\right), \quad A_3 = \frac{m^2}{K_e(M+m)^2}$$

$$A_4 = \frac{1}{2m(M+m)}, \quad \omega_n = \sqrt{\frac{K_e(M+m)}{Mm}}, \quad \xi = \frac{C_e}{2} \sqrt{\frac{M+m}{K_e Mm}}$$

$$\omega_d = \omega_n \sqrt{1 - \xi^2}$$

The parameters of the IDM and friction model for the simulation model are listed in Table 2.

TABLE 2. Parameters of IDM and friction model

Symbol	Parameters	Value (Units)
l_r	Length of Terfenol-D rod	80 mm
A_r	Areas of Terfenol-D rod	50.24 mm ²
A_m	Areas of magnetic field	157 mm ²
N	Turns of coil	880
m_l	Slider mass	1.33 kg
m_2	Counter mass	0.31 kg
v_s	Stribeck velocity	1.2×10 ⁻⁴ m/s
σ_0	Average stiffness of bristles	1×10 ⁻⁶ N/m
σ_1	Damping frictional coefficient	5 N·s/m
σ_2	Viscous frictional coefficient	0.4 N·s/m
τ_c	Coulomb friction coefficient	0.5
τ_s	Sliding friction coefficient	0.3

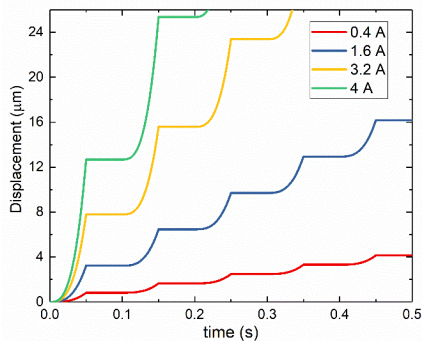


Figure 3. Displacement trajectory under different driving current

Using Equation (13) and the parameters from Table 2, we can predict the step-size of the MS-IDM. Figure 3 shows the motion trajectory curves of the IDM, when the operation frequency is 10 Hz, and the driving current are 0.4, 1.6, 3.2 and 4 A, respectively,

4. EXPERIMENT

To test the performance of the proposed in-pipe IDM, an experimental setup has been built (shown in Figure 3). The 0-1 V saw-tooth signal is generated by dSPACE platform, and amplified into 0-4 A current by AE-7224. The displacement of the IDM is measured a laser sensor with 120 nm resolution. The motion trajectory is recorded by Control Desk software, the analog data from the laser sensor and current sensor are sampled by the ADC channel of DS1103 with 12-bit sampling accuracy.

In the experiment, operation frequency range, the minimum and maximum step-size are tested. According to the linear working region set in section 2.2, the range of driving current can be determined as 0.4-4 A.

5. RESULTS AND DISCUSSIONS

Figure 5 shows the IDM's simulation and experimental displacement results. The working frequency is 10 Hz. In Figure 5, the simulation curve is smoother than the experimental curve, that is due to the inconsistent roughness of the guider surface. Hence, the IDM generates some vibration in the slip-stick process. The average error between the prediction and actual step-size is 52 nm, which provides that the given model can accurately predict the step-size of the IDM.

Figure 6 shows the displacement of the IDM on different driving currents. As shown in Figure 6a, when driving current is 0.4 A, the IDM has a minimum step-size of 780 nm, while when the driving current increased to 4 A, the step-size is 12.7 μm (shown in Figure 6b). With the increasing driving current, the change of step-size is nonlinear. The performance of Terfenol-D rod, the friction force and the system parameters all make contributions to this nonlinearity.

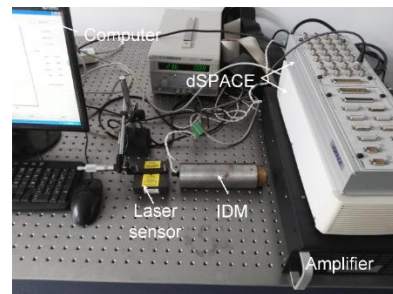


Figure 4. Experimental system to test the IDM's performance

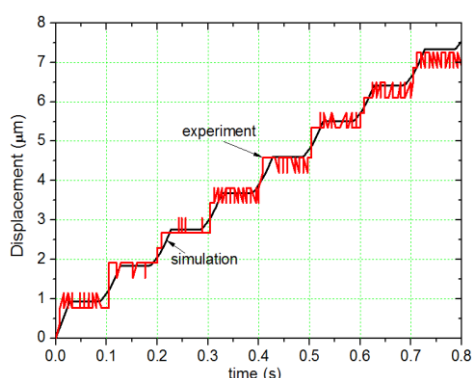
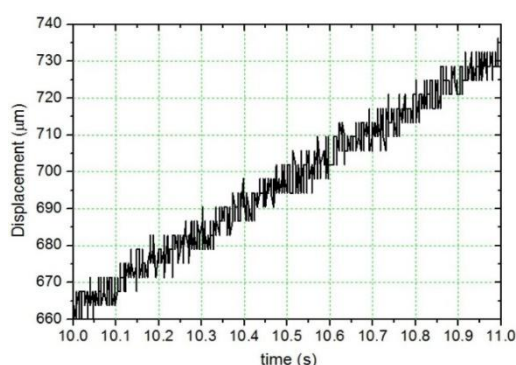
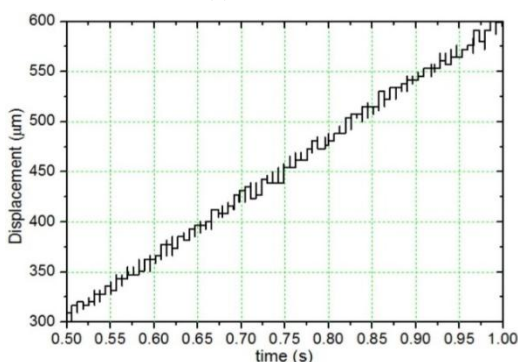


Figure 5. Comparison of simulation and experimental data



(a) $I = 0.4$ A

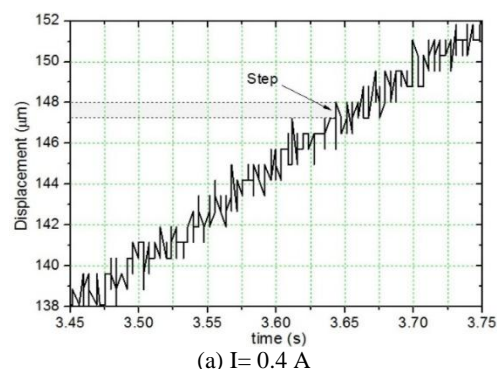


(b) $I = 4$ A

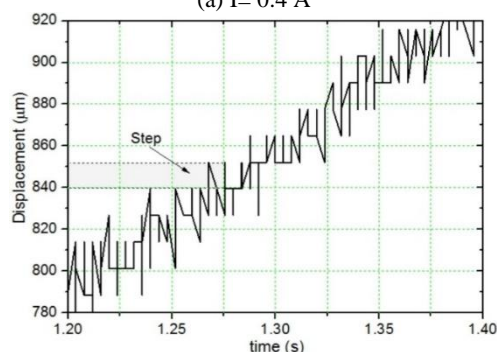
Figure 6. Comparison of simulation and experimental data

When applying a 4 A current, the Terfenol-D rod will generate a maximum magnetostriction, and which means the maximum step-size of the IDM is $12.7 \mu\text{m}$.

The motion trajectories of the MS-IDM at 20 and 120 Hz working frequency are shown in Figure 7. When the working frequency is 20 Hz, the IDM products a clear “step” at each move (see Figure 7a). But when increasing of the operational frequency, distortions gradually come out of the motion processing. There are two reasons for this phenomenon. Firstly, the inductance effect of the driving coil makes the movement response lag behind the excitation signal.



(a) $I = 0.4$ A



(b) $I = 4$ A

Figure 7. Comparison of simulation and experimental data

Secondly, the motor friction force increases with its decreasing speed. When the operation frequency reaches to 120 Hz, shown in Figure 7b, the motion trajectory became a straight line. It means that the IDM cannot work at the mode of stick-slip [8]. So, 120 Hz is the maximum working frequency of the magnetostrictive IDM.

6. CONCLUSIONS

In this study, an in-pipe magnetostrictive IDM, characterized by compact structure, was presented. In order to reduce the device size, we integrated the guide rail and the actuator housing together. An accurate mechanical model of the IDM was presented to obtain its motion equations. By resolving the motion equations, the solution of step-size was obtained. Finally, through the experiments, the performances of the in-pipe IDM were tested and the prediction model was testified. The properties of designed IDM are given as follows,

- (a) Working frequency: 10-120 Hz.
- (b) Driving current: 0.4-4 A.
- (c) Step-size resolution: 740 nm.

7. ACKNOWLEDGEMENT

This work is supported by the Natural Science Foundation of China (grant no.51165035), the Science

and Technology Project of Jiangxi Province Education Department of China (grant no.GJJ160115).

8. REFERENCES

1. Belly, C., Claeysen, F., Le Letty, R. and Porchez, T., "Benefits from amplification of piezo actuation in inertial stepping motors and application for high-performance linear micro motors *Proceeding of Actuator*, Vol. 1, (2010),1-4.
2. Zesch, W., Buechi, R., Codourey, A. and Siegwart, R.Y., "Inertial drives for micro-and nanorobots: Two novel mechanisms", in *Microrobotics and Micromechanical Systems*, International Society for Optics and Photonics. Vol. 2593, (1995), 80-89.
3. Cheshmehbeigi, H.M. and Khanmohamadian, A., "Design and simulation of a moving-magnet-type linear synchronous motor for electromagnetic launch system", *International Journal of Engineering-Transactions C: Aspects*, Vol. 30, No. 3, (2017), 1183-1188.
4. Kurosawa, M. and Ueha, S., "Hybrid transducer type ultrasonic motor", *IEEE transactions on ultrasonics, ferroelectrics, and frequency control*, Vol. 38, No. 2, (1991), 89-92.
5. Sayyaadi, H. and Zakerzadeh, M., "Nonlinear analysis of a flexible beam actuated by a couple of active sma wire actuators", *International Journal of Engineering, Transactions A: Basics*, Vol.25, No. 3, (2012), 249-264.
6. Nosier, A. and ROUHI, M., "Three dimensional analysis of laminated cylindrical panels with piezoelectric layers", *International Journal of Engineering, Transactions B: Applications*, Vol.19, No.1, (2006), 61-72.
7. Yuan, M., "Compact and efficient active vibro-acoustic control of a smart plate structure", *International Journal of Engineering, Transactions B: Applications*, Vol. 29, No. 8, (2006), 1068-1074.
8. Edeler, C., Meyer, I. and Fatikow, S., "Modeling of stick-slip micro-drives", *Journal of Micro-Nano Mechatronics*, Vol. 6, No. 3-4, (2011), 65-87.
9. Hattori, S., Hara, M., Nabae, H., Hwang, D. and Higuchi, T., "Design of an impact drive actuator using a shape memory alloy wire", *Sensors and Actuators A: Physical*, Vol. 219, (2014), 47-57.
10. Ueno, T. and Higuchi, T., "Miniature magnetostrictive linear actuator based on smooth impact drive mechanism", *International Journal of Applied Electromagnetics and Mechanics*, Vol. 28, No. 1, 2, (2008), 135-141.
11. Okamoto, Y., "The development of a smooth impact drive mechanism (sidm) using a piezoelectric element", *Konica Minolta Technol. Rep.*, Vol. 1, (2004), 23-26.
12. Eigoli, A.K. and Vossoughi, G., "Dynamic modeling of stick-slip motion in a legged, piezoelectric driven microrobot", *International Journal of Advanced Robotic Systems*, Vol. 7, No. 3, (2010), 201-208.
13. Zhou, J.J., Pan, Y.L. and Huang, M., "A novel magnetostrictive drive rotary motor", in *Solid State Phenomena*, Trans Tech Publ. Vol. 121, (2007), 1203-1206.
14. Kim, W.-j. and Sadighi, A., "A novel low-power linear magnetostrictive actuator with local three-phase excitation", *IEEE/ASME Transactions on Mechatronics*, Vol. 15, No. 2, (2010), 299-307.
15. Zhang, Z.G., Ueno, T. and Higuchi, T., "Magnetostrictive actuating device utilizing impact forces coupled with friction forces", in *Industrial Electronics (ISIE)*, 2010 IEEE International Symposium on, IEEE., (2010), 464-469.
16. Yang, C.-F., Jeng, S.-L. and Chieng, W.-H., "Motion behavior of triangular waveform excitation input in an operating impact drive mechanism", *Sensors and Actuators A: Physical*, Vol. 166, No. 1, (2011), 66-77.
17. Engdahl, G. and Mayergoyz, I., "Handbook of giant magnetostrictive materials (academic, new york, 2000)", *Google Scholar*, 209-217.
18. Zheng, X. and Liu, X., "A nonlinear constitutive model for terfenol-d rods", *Journal of applied physics*, Vol. 97, No. 5, (2005), 1-8.
19. Kang, C.-Y., Yoo, K.-H., Ko, H.-P., Kim, H.-J., Ko, T.-K. and Yoon, S.-J., "Analysis of driving mechanism for tiny piezoelectric linear motor", *Journal of electroceramics*, Vol. 17, No. 2-4, (2006), 609-612.
20. Liu, Y., Li, J., Hu, X., Zhang, Z., Cheng, L., Lin, Y. and Zhang, W., "Modeling and control of piezoelectric inertia-friction actuators: Review and future research directions", *Mechanical Sciences*, Vol. 6, No. 2, (2015), 95-107.
21. Fung, R.-F., Han, C.-F. and Ha, J.-L., "Dynamic responses of the impact drive mechanism modeled by the distributed parameter system", *Applied Mathematical Modelling*, Vol. 32, No. 9, (2008), 1734-1743.

Design, Modeling and Experiments of An In-pipe Magnetostrictive Impact Drive Mechanism

R. Zhao^{a,b}

^a Jiangxi Province Key Laboratory of Precision Drive & Control, Nanchang Institute of Technology, Nanchang, China

^b School of Electrical Engineering, Hebei University of Technology, Tianjin, China

P A P E R I N F O

چکیده

Paper history:

Received 27 August 2016

Received in revised form 14 February 2018

Accepted 14 February 2018

Keywords:

In-pipe Motor

Impact Drive Mechanism

Magnetostrictive Materials

Inertia Impact Principle

Precision Positioning

این مقاله مکانیزم تاثیر مگنتواستراکتیو لوله ها را ارائه میدهد. جهت تخمین کارایی مدل دینامیکی براساس ماده مگنتواستراکتیو توسعه یابد. لذا سیستم تجربی بر پایه آزمایش ها ساخته شد تا کارایی حرکت دینامیکی مورد آزمایش قرار گیرد. نتایج تجربی و سیموله شده نشان میدهد که مدل بطور دقیق می تواند با اندازه اینکرومنت پیش گویی نماید. تکرار پذیری از ۱۰ الی ۱۲۰ هرتز و با اندازه اینکرومنت ۷۴۰ نانومتر قابل اجراست. کارایی الگو مگنتواستراکتیو بصورت خطی با دقت بالا مورد قبول می باشد.

doi: 10.5829/ije.2018.31.05b.08
